Broadband THz detection by YBaCuO Josephson junctions having finite capacitance

EKATERINA A. MATROZOVA, LEONID S. REVIN,
Institute for Physics of Microstructures of RAS, GSP-105, Nizhny Novgorod, 603950, Russia
Superconducting Nanoelectronics Laboratory, Nizhny Novgorod State Technical University, n.a. R.E. Alekseev, 603950 Nizhny Novgorod, RUSSIA

Abstract:—Broadband classical detection of THz radiation by a YBaCuO Josephson junction was studied on the basis of resistively-capacitively shunted junction model. Numerical simulation was based on the parameters of the samples experimentally studied in other works at nitrogen temperatures. It is shown that taking into account the damping of the Josephson junction becomes essential for high frequencies of external signal. The absolute value of responsivity decreases as junction capacitance increases. Damping parameter also influences the choice of optimal IC and RN parameters.

Keywords:—YBaCuO Josephson junction, broadband detector, responsivity, RCSJ model.

Received: May 14, 2022. Revised: October 8, 2022. Accepted: November 16, 2022. Published: December 31, 2022.

1. Introduction

HIGHLY sensitive microwave detectors are essential for biomedical research, security control and atmospheric monitoring. In this field superconducting devices such as Josephson broadband and selective detectors, mixers, Hilbert spectrometers offer a viable option. In contrast to conventional niobium devices high-temperature superconductors (HTSC) have higher operating temperatures and wider THz frequency response. Grain-boundary Josephson junctions (JJs) have already proven their advantages [1]-[3]. Table I shows parameters of Josephson detectors obtained in different works for nitrogen temperatures.

The analysis and comparison of the results of Table I is difficult due to some difference in the working temperature and the frequency of external influence. Moreover, not all works contain information about for what type of power, incident or absorbed, the value of responsivity r_V was obtained. In addition, in paper [4] a frequency selective responsivity has been measured instead of a broadband one. Nevertheless, for a numerical analysis as close to reality as possible we used the sample parameters from these works.

To model the broadband response of a non-hysteretic junction a resistively shunted junction model is usually employed [9]-[12]. To simulate such systems quantitatevly we will use a resistively and capacitively shunted junction (RSCJ) model even though the junction does not exhibit hysteresis in its current-voltage characteristics.

The aim of this paper is to study the influence of the Josephson junction finite capacitance on the characteristics of the broadband response for different frequencies of external signal, different $I_C R_N$ product and optimal I_C and R_N parameters at 77 K.

2. Numerical Results

The investigation was performed using the RSCJ model where the junction phase φ with a critical current I_C, capacitance C, resistance R_N is described by the stochastic differential equation [13]-[14]

Table I. Experimental parameters of YBaCuO bicrystal detectors obtained in different works. Here r_V is the responsivity.

T [K]	F_{mw} [GHz]	I_C [μA]	R_N [Ω]	$I_C R_N$ [mV]	r_V [V/W]	Ref.
77	614	80	1.5	0.12	300	[3]
75	690	220	4.1	0.9	16000	[4]
80	500	28	4.8	0.13	20000	[5]
77	300	98	5.8	0.57	170	[6]
77	200	60	1.2	0.072	–	[7]
77	400	510	1.0	0.51	–	[8]

$$C\frac{dV}{dt}+\frac{V}{R_N}+I_C\sin\varphi+I_{mw}\sin(F_{mw}2\pi t)+I_F=I_B \qquad (1)$$

where voltage V is defined as the derivative $d\varphi/dt\cdot 2\pi\Phi_0$ with the magnetic flux quantum Φ_0; thermal fluctuations I_F are treated as white Gaussian noise with zero mean and correlation function $\langle I_F(t)I_F(t+\tau)\rangle = (k_B T) / (\pi R_N)\ \delta(\tau)$. A simple harmonic signal of amplitude I_{mw} and frequency $F_{mw} = \omega_{mw}/2\pi$ describes external radiation with power $P_{mw} = I_{mw}^2 R_N / 2$.

The receiving characteristics of JJ was analyzed in the bias current regime to study the responsivity r_V in the broadband detection mode. That is, at the bias current near the critical one the voltage increment is associated with the change in the power of the incident signal.

For clarity, Fig. 1a shows current-voltage characteristic and differential resistance R_D for the experimental parameters from [3]: T = 77 K, I_C = 80 μA, R_N = 1.5 Ω. Determining the capacitance of the Josephson junction, and, accordingly, the damping parameter $\alpha = 1/R_N\ (\hbar/(2eI_C C))^{-2}$ is quite difficult task. Nevertheless, estimations can be made based on the fitting of IV curves for different temperatures. For the experimental current-voltage characteristics from Fig. 3 of [3] the capacitance value of JJ obtained from the fitting is $C \approx 190$ fF ($\alpha \approx 4$ for T = 77 K). While for IVs from Fig. 1 of [15] $C \approx 2$ fF, and it can be assumed that for this case α will be no more than 3 for nitrogen temperature. Figure 1 was obtained for two different damping parameters: for the case of overdumped junction with α = 50 (curve marked with 1) and for α = 3 (curve marked with 2). While the current-voltage characteristics and R_D for the two cases are almost the same, the response ΔV to a small external signal with F_{mw} = 614 GHz; P_{mw} = 10 nW is different (Fig. 1b). This effect will be described in more detail further.

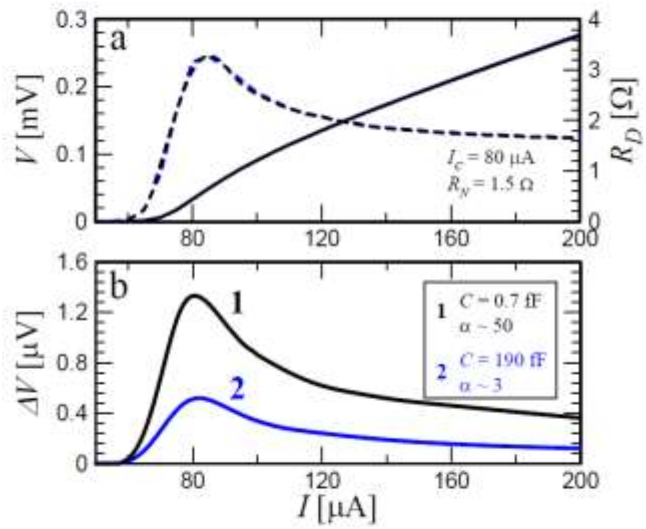

Fig. 1 a) Left (solid curve): IV characteristics for I_C = 80 μA, R_N = 1.5 Ω, T = 77 K without an external signal. Right (dashed curve): Differential resistance R_D. Curves for the two alpha values α = 3, α = 50 are almost the same. (b) Response ΔV to an external signal with F_{mw} = 614 GHz; P_{mw} = 10 nW depending on the bias current for two values of α.

Choosing an optimal bias I_B, we get the maximum voltage response to the external signal at a given power. Then responsivity is defined as derivation $r_V = dV / dP_{mw}$. The voltage amplitude of the response ΔV is a linear function of the radiation power at low values of this power (the inset of Fig. 2). Thus, the responsivity is constant and has a maximum value for small external signals, Fig. 2. Note that for the case of α = 50 the max r_V is ~ 2.2 times greater than for the case of α = 3. At the same time, the responsivity for curve 1 decreases faster with increasing power than for curve 2. To describe the $r_V(P_{mw})$ dependency we will use the upper limit of the power dynamic range P_S defined as the power at which the detector responsivity decreases by a factor of two.

Let us examine the influence of damping on the value of the maximum responsivity for different frequency F_{mw} (Fig. 3). It is convenient to perform this using the parameters of two detectors with different $I_C R_N$ product from Table I. In the absent of fluctuations and for the normalized frequency $\Omega_{mw} = F_{mw} / F_C > 1$, where F_C is the characteristic frequency, the analytical formula for the broadband responsivity was obtained in the framework of the resistively shunted (RSJ) model [9]:

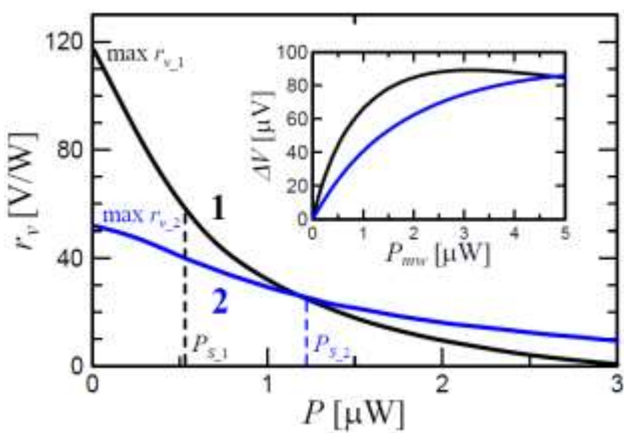

Fig. 2 Voltage responsivity versus P_{mw}. Max r_V and P_S indicate the maximum responsivity at low power and the upper limit of the power dynamic range, respectively. The inset: response amplitude ΔV vs. external radiation power with a frequency of F_{mw} = 614 GHz at temperature of 77 K. Detector parameters are the same as for Fig. 1.

$$r_V = \frac{R_D}{2I_C R_N} \cdot \frac{1}{\Omega_{mw}^2} \tag{2}$$

where $\Omega_{mw} = F_{mw} / (I_C R_N \cdot 2e/\hbar)$.

Figure 3 shows the data for $I_C R_N$ = 0.12 mV (curves marked with 2) and normalized frequencies Ω_{mw} from 3 to 17. The result for α = 50 is in complete agreement with the analytical formula. At the same time, a decrease in damping leads to a stronger $r_V(F_{mw})$ dependence. A similar dependence on α was observed in the study of Shapiro steps [16]. In this case, the 0th Shapiro step, that is, the critical current, can be approximately considered as the broadband current response of the Josephson junction in the voltage bias regime. It has been shown that the $I_C(P)$ dependence is slower for lower damping, which means that the responsivity dI_C/dP decreases with decreasing α. This result can be explained by the increase of the junction admittance in the simple RC-model. The frequency at which the influence of α becomes significant is determined by the condition: $F_{mw} \geq F_P^2 / F_C$, where $F_P = (2eI_C/\hbar C)^{-2}$ is the plasma frequency. So for curve 2 in Fig. 3 for α = 3 this frequency corresponds to 550 GHz. For α = 2 - 230 GHz and for α = 1 - 60 GHz.

For $I_C R_N$ = 0.9 mV (curves marked with 1) the normalized frequencies Ω_{mw} are from 0.1 to 2. For $\Omega_{mw} > 1$ the dependence is similar to the one discussed above. For low frequencies the responsivity dependence is slower than $1/\Omega_{mw}^2$. In this region, the difference in r_V values for different damping is small and is

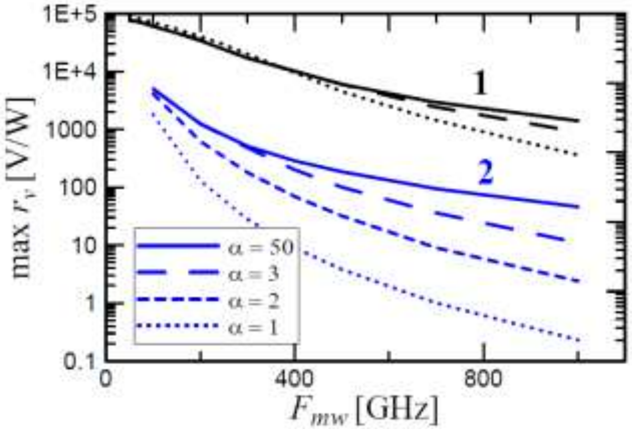

Fig. 3 Maximum responsivity depending on the frequency F_{mw} for $I_C R_N$ = 0.9 mV (curves marked with 1) and for $I_C R_N$ = 0.12 mV (marked with 2) from Table I. Solid curves - α = 50, long dashed curves - α = 3, short dashed curves - α = 2, dotted curves - α = 1.

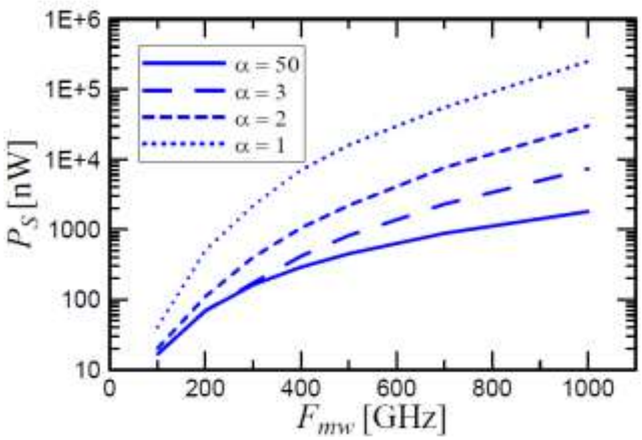

Fig. 4 The upper limit of the power dynamic range on the frequency F_{mw} for $I_C R_N$ = 0.12 mV from Table I. Solid curves - α = 50, long dashed curves - α = 3, short dashed curves - α = 2, dotted curves - α = 1.

associated with a larger value of R_D for smaller α.

The dependence of the upper limit of the power dynamic range on frequency for different α shows an inverse character, Fig. 4. In the $\Omega_{mw} > 1$ limit P_S - value increases with increasing frequency and decreasing α.

Now let us consider the task of finding the optimal I_C and R_N parameters for a given values of $I_C R_N$ at a temperature of 77 K to obtain maximum broadband responsivity. Technologically this task can be solved by adjusting the geometry of the junction, in particular by the film thickness. I_C and R_N

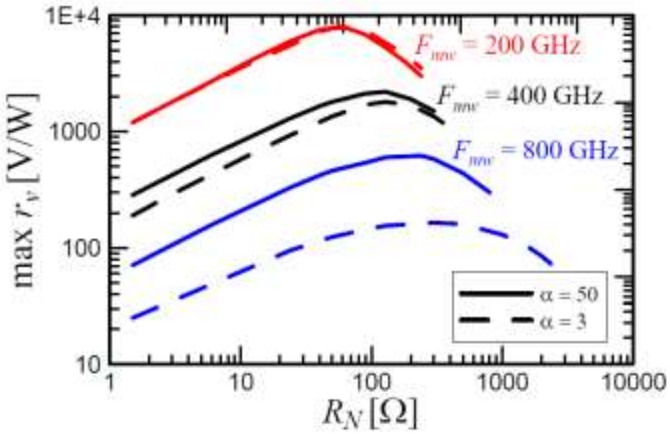

Fig. 5 The dependence of max r_V on the normal resistance at constant $I_C R_N$ = 0.12 mV for different F_{mw}. Solid curves - α = 50, long dashed curves - α = 3.

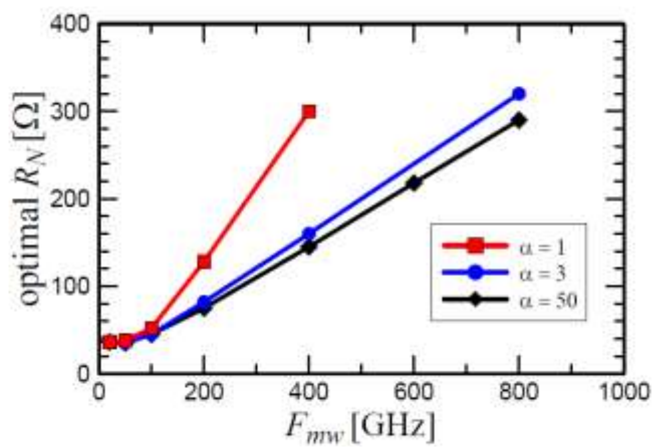

Fig. 6 The dependence of optimal R_N on the frequency F_{mw} for $I_C R_N$ = 0.12 mV and different α.

parameters can also be changed by low-temperature annealing of bicrystal junctions in ozone atmosphere [17], annealing in atomic oxygen [18] and by oxygen aging [19]. In [10] the results of numerical simulations for the responsivity as well as the noise-equivalent power (NEP) was obtained in the framework of RSJ model with thermal noise. There, the r_V-values have their maximum at $R_N \sim (\hbar I_C R_N) / (2ekT)$ for normalized frequencies $\Omega_{mw} < 1$ and should have them at $R_N \sim (\Omega_{mw}\, \hbar I_C R_N) / (2ekT)$ for large $\Omega_{mw} \geq 1$. Simulation for α = 50 shows a similar result, Fig. 5. As α decreases, the optimal R_N value shifts to the right, and the responsivity maximum becomes flatter.

Figure 6 demonstrates optimal R_N -value for the greatest responsivity versus frequency for different α. It can be seen that the optimal R_N is the same for different damping in low frequency region $F_{mw} < F_C$ while in high frequency region the $R_N(F_{mw})$ dependence is almost linear with different slopes.

3. Conclusions and Discussion

We have shown that taking into account finite damping can lead to a change in the $r_V(F_{mw})$ dependence even for $\alpha = 3$. In the high frequency region $F_{mw} \geq F_P^2 / F_C$ the absolute value of responsivity decreases as α decreases. At the same time, the dependence of the upper limit of the power dynamic range on damping is inverse. For a more detailed analysis, it is required to investigate the NEP(α) dependence and, as a consequence, to investigate the power dynamic range $D = P_S / NEP\ (\Delta F)^{-2}$, where ΔF is the frequency band in which the output signal is measured.

Damping parameter also influences the choice of I_C and R_N for optimal broadband detection. As α decreases, the recommendations shift to the region of higher normal resistances and lower critical currents compared to the overdamped junction.

Accounting for finite damping is important even when analyzing the characteristics of HTSC detectors at nitrogen temperatures. The RCSJ model should be applied for frequencies F_{mw} above F_P^2 / F_C.

References

[1] O. Volkov, V. Pavlovskiy, I. Gundareva, R. Khabibullin, Y. Divin, "In Situ Hilbert-transform spectral analysis of pulsed terahertz radiation of quantum cascade lasers by high-Tc Josephson junctions," IEEE Trans. Terahertz Sci. Technol., vol. 11, pp. 330-338, 2021.

[2] V.V. Pavlovskiy, I.I. Gundareva, O.Y. Volkov, Y.Y. Divin, "Wideband detection of electromagnetic signals by high-Tc Josephson junctions with comparable Josephson and thermal energies," Appl. Phys. Lett., vol. 116, p. 082601, 2020.

[3] J. Du, K. Smart, L. Li, K.E. Leslie, S.M. Hanham, D.H.C. Wang, C.P. Foley, F. Ji, X.D. Li, D.Z. Zeng, "A cryogen-free HTS Josephson junction detector for terahertz imaging," Supercond. Sci. Technol., vol. 28, p. 084001, 2015.

[4] M.V. Lyatti, D.A. Tkachev, Yu.Ya. Divin, "Signal and noise characteristics of a terahertz frequency-selective $YBa_2Cu_3O_{7-x}$ Josephson detector," Techn. Phys. Lett., vol. 32, pp. 860-863, 2006.

[5] G.A. Ovsyannikov, I.V. Borisenko, K.Y. Constantinian, Y.V. Kislinski, A.A. Hakhoumian, N.G. Pogosyan, T. Zakaryan, N.F. Pedersen, J. Mygind, N. Uzunoglu, E. Karagianni, "Bandwidth and noise of submillimeter wave cuprate bicrystal Josephson junction detectors," IEEE Trans. Appl. Supercond., vol. 15, pp. 533-536, 2005.

[6] M.A. Tarasov, E.A. Stepantsov, A.S. Kalabukhov, M.Yu. Kupriyanov, D. Winkler, "Temperature sensitivity and noise of an HTSC Josephson detector on a sapphire bicrystal substrate at 77 K," J. Exp. Theor. Phys. Letters, vol. 86, pp. 718-720, 2007.

[7] M. Kawasaki, P. Chaudhari, A. Gupta, "1/f noise in $YBa_2Cu_3O_{7-\delta}$ superconducting bicrystal grain-boundary junctions," Phys. Rev. Lett., vol. 68, pp. 1065-1068, 1992.

[8] M.A. Tarasov, D. Golubev, V. Shumeiko, Z. Ivanov, E.A. Stepantsov, O. Harnak, T. Claeson, "Subharmonic Shapiro steps and noise in high-Tc superconductor Josephson junctions," J. Exp. Theor. Phys. Letters, vol. 68, pp. 454-459, 1998.

[9] H. Kanter, F.L. Vernon, "Response of superconducting point contacts to high frequency radiation," Phys. Lett., vol. 35A, no.5, p. 349, 1971.

[10] A.N. Vystavkin, V.N. Gubankov, L.S. Kuzmin, K.K. Likharev, V.V. Migulin, V.K. Semenov, "S-c-S junctions as nonlinear elements of microwave receiving devices," Rev. Phys. Appl., vol. 9, p. 79, 1974.

[11] Y.Y. Divin, V.V. Pavlovskii, D.A. Tkachev, O.Y. Volkov, V.N. Gubankov, K. Urban, "Broadband THz detection by high-Tc Josephson junctions," Joint 31st International Conference on Infrared Millimeter Waves and 14th International Conference on Teraherz Electronics, p. 345, 2006.

[12] V.V. Pavlovskiy, Y.Y. Divin, "Limiting Characteristics of Classical Josephson Detector," Journ. Comm. Tech. Electronic., vol. 64, pp. 1003-1010, 2019.

[13] M.J. Stephen, "Noise in a driven Josephson oscillator," Phys. Rev., vol. 186, pp. 393-397, 1969.

[14] K.K. Likharev, "Dynamics of Josephson junctions and circuits," New York: Gordon and Breach Science Publishers, Chap. 13, 1986.

[15] I. Gundareva, V. Pavlovskiy, Y. Divin, "High-Tc Josephson junctions as quasiclassical THz detectors," IEEE Trans. Appl. Supercond., vol. 28, p. 1800105, 2018.

[16] Y. Mizugaki, J. Chen, K. Nakajima, T. Yamashita, "Numerical evaluation for the high-frequency response of Josephson junctions having finite capacitance," Jpn. J. Appl. Phys., vol. 37, pp. 5971-5972, 1998.

[17] I.I. Gundareva, O.Y. Volkov, M.V. Lyatti, Y.Y. Divin, V.N. Gubankov, V.V. Pavlovskiy, "Evolution of electrical and electrodynamic properties of $YBa_2Cu_3O_{7-x}$ bicrystal Josephson junctions with oxygen loading," IEEE Trans. Appl. Supercond., vol. 21, pp. 147-150, 2011.
[18] M.A. Tarasov, E.A. Stepantsov, M. Naito, A. Tsukada, D. Winkler, A.S. Kalabukhov, M.Yu. Kupriyanov, "Superconducting weak bonds at grain boundaries in MgB_2," J. Exp. Theor. Phys., vol. 105, pp. 636–641, 2007.
[19] M.V. Lyatti, U. Poppe, Y.Y. Divin, "Electrical transport and noise properties of [100]-tilt $YBa_2Cu_3O_{7-x}$ grain-boundary junctions with high IcRn Product," IEEE Trans. Appl. Supercond., vol. 17, pp. 314-317, 2007.

Contribution of individual authors to the creation of a scientific article (ghostwriting policy)

Author Contributions: Please, indicate the role and the contribution of each author:
Example
Ekaterina Matrozova carried out the simulation and the optimization.
Leonid Revin has implemented the numerical scheme in C and general guidance.

Sources of funding for research presented in a scientific article or scientific article itself

The work was supported by the Russian Science Foundation (Project No.20-79-10384).

Creative Commons Attribution License 4.0 (Attribution 4.0 International , CC BY 4.0)